

See discussions, stats, and author profiles for this publication at: <https://www.researchgate.net/publication/282184427>

Dynamic Behavior of Novel Vertical Axis Tidal Current Turbine: Numerical and Experimental Investigations

Conference Paper · June 2005

CITATIONS

9

READS

20

5 authors, including:



Domenico Coiro

University of Naples Federico II

58 PUBLICATIONS 208 CITATIONS

[SEE PROFILE](#)



Fabrizio Nicolosi

University of Naples Federico II

60 PUBLICATIONS 236 CITATIONS

[SEE PROFILE](#)



Agostino De Marco

University of Naples Federico II

40 PUBLICATIONS 118 CITATIONS

[SEE PROFILE](#)

Some of the authors of this publication are also working on these related projects:



Risk Analysis for Airplane operating near Wind Farms [View project](#)

Dynamic Behavior of Novel Vertical Axis Tidal Current Turbine: Numerical and Experimental Investigations

D.P. Coiro, F. Nicolosi, A. De Marco, S. Melone, F. Montella
Dipartimento di Progettazione Aeronautica (DPA), University of Naples "Federico II"
Naples, Italy

ABSTRACT

This paper presents a summary of the recent work done by the authors regarding the design, construction and test of a novel patented vertical axis and variable pitching blade hydro turbine, named *KOBOLD*, capable of harnessing clean and renewable energy from marine tidal currents. The *KOBOLD* turbine, currently moored in Messina Strait, between mainland Italy and Sicily island, is the only existing turbine of this type devoted to exploit tidal currents, and has a 25% global system efficiency. Theoretical analysis and numerical prediction performances have been compared and validated with experimental test results on both model and real scale turbines. Moreover, the recent activities in terms of numerical and experimental investigations on vertical axis hydro turbines are presented.

KEY WORDS

Vertical-Axis-Hydro-Turbine; Variable Pitch; Curved Airfoil; Double-Multiple-Streamtube; Vortex; Flow Curvature; Tidal Energy.

INTRODUCTION

Marine current energy is a type of renewable energy resources that has been less exploited respect to wind energy. Only in the last few years, some countries have devoted funds to the researches aimed to develop tidal current power stations. Tidal current turbines, as in the wind community, can be divided into vertical and horizontal axis. Although the horizontal axis turbines have been more popular than vertical axis ones for wind energy exploitation, the vertical axis turbines could present significant advantages for tidal current exploitation, because they are simple to built and reliable in working conditions. Therefore, at beginning of the studies, vertical axis wind turbines were taken as models for hydro-turbines. The blades of Darrieus type vertical axis wind turbines are fixed in pitch and they show good performances when the blade solidity is low and working speed is high. It is also well known that the Darrieus type turbines are impossible to start and for this reason a variable-pitch blades system can be a solution to this problem. Some prototypes with different types of pitching system have been developed around the world: the *KOBOLD* turbine in the Strait of Messina, Italy, the cycloidal turbine in Guanshan, China, the moment-

control turbine in Edinburgh University, UK and the mass-stabilized system turbine by Kirke and Lazauskas in Inman Valley, South Australia. Ponte di Archimede S.p.A. Company located in Messina, Italy, owns the patented *KOBOLD* turbine that has been developed since 1997 within the ENERMAR project; the rotor has a self-acting variable pitch blades that employ an *ad hoc* designed curved airfoil, called HLIFT18 that is cavitation-free and has high lift performance. Also the theoretical/numerical methods to predict the hydrodynamic performances of the vertical axis turbines come from the wind turbines: [Templin \(1974\)](#) developed the Single-Disk Single-Tube model and then [Strickland](#) put forward the Single-Disk Multi-Tube model. In the 1980's [Paraschivou](#) (see also [Paraschiou 2002](#)) introduced the Double-Disk Multi-Tube model (DMS). The VAWT and VAWT_DYN computer codes, based on the DMS theory, have been developed to predict the steady and dynamic performances of a cycloturbine with fixed or self-acting variable pitch straight-blades. Numerical results have been compared with two sets of experimental data: one set is obtained from wind tunnel test on scaled model and another set is relative to field data of the *KOBOLD* prototype. To overcome the limits of the DMS model, a 3D vortex method has been used to analyse the performances when solidity is high and comparison with the DMS codes will be presented. Furthermore detailed analysis of flow curvature effect has been performed using panel method technique and the effect of this on the optimal airfoil shape will be discussed.

EXPERIMENTAL INVESTIGATIONS

The experimental data reported are divided in two parts: 1) experimental data measured in the DPA wind-tunnel of University of Naples on a small straight-bladed cycloturbine, which was designed, developed and assembled at DPA (Coiro and Nicolosi, 1998; Coiro, Nicolosi, De Marco, Melone and Montella, 2004); 2) experimental data measured in water on the *KOBOLD* prototype (real scale) (Montella and Melone, 2003). Both the DPA straight-bladed cycloturbine (later on indicated also as Model A) and the *KOBOLD* prototype (later on indicated also as Model B) will be described as follow. Both turbines have variable pitch blades with a self-acting system that is made up of two balancing mass for each blade. In this way, it is possible to move blade gravity centre in its optimal position in order to optimize the global performance of the rotor. The use of two stops makes possible to limit the pitch blade range, as shown in Figure 1.

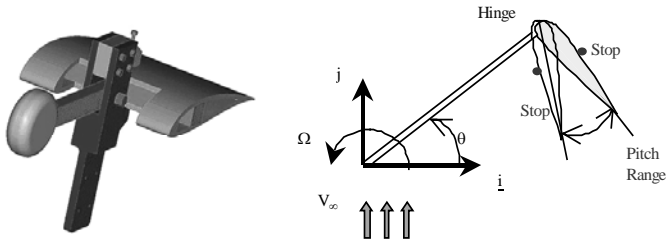


Fig. 1 - Balancing mass and blade stops

The model A in the DPA wind tunnel is shown in the Figure 2.

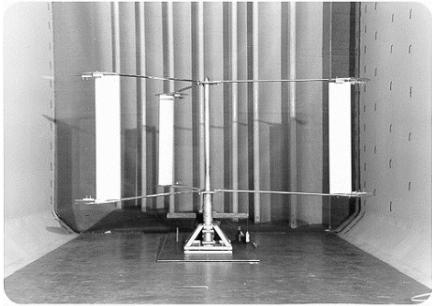


Fig. 2 - DPA straight-bladed cycloturbine (Model A)

Using different stop positions, it has been possible to test different pitch angle ranges, while using different number of blade it has been possible to take into account different solidity $\sigma = N_b c/R$ values, where N_b is the number of blades, c the blade chord and R the rotor radius. The Model A has the following geometric parameters: number of blades tested 2, 3, 4 and 6; a blade chord of 0.15 m with a NACA 0018 airfoil; blade span 0.8 m length giving an Aspect Ratio of 5.33; radius of 1.05 m; two radial arms for each blade; arm chord of 0.05 m. The *KOBOLD* prototype lies out in the Strait of Messina, close to the Sicilian shore. In this site the peak currents speed is 2 m/s (4 knots), the sea depth is 20 meters and the plant has been moored at 150 metres offshore. The current changes direction every 6 hrs and 12 minutes and the amplitude period is equal to 14 days. A high lift curved airfoil, called HLIFT18, is used for the blade sections and it has been purposely designed at DPA to be cavitation free and to optimise the turbine performances. The use of a curved airfoil is one of the innovative aspects of this turbine. All existing vertical axis turbines employ symmetrical airfoils while it has been shown within the development of this project that, with a proper design, the curved airfoil works much better than symmetrical one. Two arms sustain each blade and the arms have been streamlined using another *ad hoc* designed symmetrical airfoil that minimizes drag. Another innovative aspect of the *KOBOLD* turbine is the unique blade oscillation principle around hinge axis governed just by hydrodynamic and centrifugal forces. Thanks to this very simple way of oscillating, the turbine is able to start rotating autonomously showing high starting torque also with electrical load connected, avoiding, in this way, the need of any starting devices; then it is capable of speeding up to the design angular rate, overcoming the typical starting difficulties of similar vertical axis turbines used in wind energy field (Darrieus, for example). The ENERMAR plant is composed by the turbine rotor hanging under a floating buoy that contains the remaining mechanical and electrical parts to deliver energy to the electrical network, as shown in Figure 3. The rotor has a diameter of 6 meters with 6 radial arms holding three blades with 5 meters span and with a chord of 0.4 m employing the HLIFT18 airfoil leading to an aspect ratio of 12.5 and to a solidity $\sigma = 0.4$. An international patent owned by "Ponte di Archimede S.p.A" covers *KOBOLD* turbine project.



Fig. 3 - *KOBOLD* plant picture

The acquisition data system is made up of a torque-meter, a tidal current speed-meter and a RPM counter all connected to a PLC that converts analog signals to digital data transferring them to a PC. A data handling software has been developed to monitor in real time the acquired data. Figure 4 shows some components of the acquisition data system. The PLC acts also as electrical load controller to keep the turbine working always at its maximum efficiency independently from current speed.

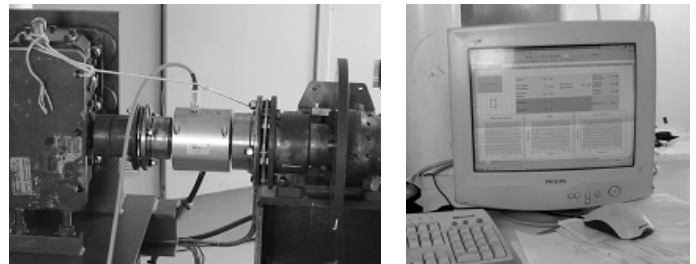


Fig. 4 - The torque-meter and the real-time data acquired by the PC

NUMERICAL INVESTIGATIONS: DOUBLE MULTIPLE STREAMTUBE MODEL

In order to analyse the flow field around a vertical axis turbine, the Double Multiple Streamtube (DMS) model has been used. DMS model is an evolution of the previous "*momentum models*": single streamtube model (Templin,1974), multiple streamtube model and double streamtube model (Strickland,1986). DMS model (Paraschivoiu, 2002) assumes that the flow through the rotor can be modelled by examining the flow through more streamtubes and the flow disturbance, produced by the rotor, is determined by equating the aerodynamic forces on the turbine rotor to the time rate of change in momentum through the rotor. In the DMS model the flow velocities vary in both the upwind and downwind regions of the streamtube as well as varying from streamtube to streamtube. So DMS is able to analyse the interference between the downwind blade and the upwind blade's wake in order to evaluate more accurately the local value of the velocity and the instantaneous blade load. As shown in Figure 5, the rotor is modelled as a series of elementary streamtubes and each streamtube is modelled with two actuator disks in series. Across the actuator disk the pressure drops and this drop is equivalent to the stream wise force dF on the actuator disk divided by the actuator disk area dA . θ is the blade angular position, subscript "u" for the upwind position and subscript "d" for the downwind position.

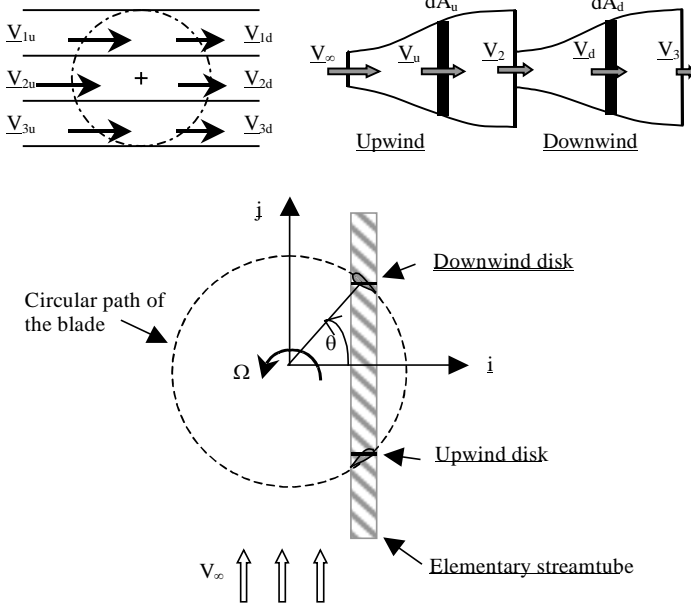


Fig. 5 - Double Multiple Streamtube model

The elementary force dF_u and dF_d , respectively on the upwind (u) and downwind (d) disk, given by the momentum principle, are

$$dF_u = \rho V_u dA_u (V_\infty - V_2) \quad \text{where} \quad V_2 = V_\infty (1 - 2a_u) \quad (1)$$

$$dF_d = \rho V_d dA_d (V_2 - V_3) \quad \text{where} \quad V_3 = V_\infty [1 + 2(a_u - a_d)] \quad (2)$$

V_d , which is the velocity on the downwind actuator disk, is influenced by the velocity V_u on the upwind actuator disk. The elementary forces dF on the actuator disks may be calculated with the Blade Element Theory. The upwind and downwind interference factors are defined as

$$a_u = \frac{V_\infty - V_u}{V_\infty} \quad a_d = \frac{V_\infty - V_d}{V_\infty} \quad (3)$$

and the mathematical problem can be reduced to the calculation of a_u and a_d . Because of non-linearity of the equations, the problem must be resolved iteratively. If rotor blades have a fixed pitch angle or an assigned pitch variation (i.e. sinusoidal like in Pinson, cycloidal, etc.), the mathematical model is reduced, for each elementary streamtube, to an equation for the momentum balance for the upwind actuator disk and an equation for the momentum balance for the downwind actuator disk.

$$\begin{cases} a_u (1 - a_u) = \frac{1}{|\sin \theta_u|} \frac{\sigma}{8\pi} \left(\frac{V_{Ru}}{V_\infty} \right)^2 \{ C_{Lu} \sin [\theta_u + \alpha_{\tan u}] \\ - C_{Du} \cos [\theta_u + \alpha_{\tan u}] \} \\ (1 - a_d)(a_d - 2a_u) = \frac{1}{|\sin \theta_d|} \frac{\sigma}{8\pi} \left(\frac{V_{Rd}}{V_\infty} \right)^2 [C_{Ld} \sin (\theta_d + \alpha_{\tan d}) \\ - C_{Dd} \cos (\theta_d + \alpha_{\tan d})] \end{cases} \quad (4)$$

Where V_R is the relative velocity of the blade, C_L is the blade lift coefficient, C_D is the blade drag coefficient and α_{\tan} is the angle

between the relative velocity and the local tangent to the path. If rotor blades have a self-acting variable pitch angle (Kentfield, 1983; Lazauskas, 1992; Kirke and Lazauskas, 1993), it is also necessary another equation for each actuator disk: the hinge moment equilibrium. In this case, in fact, the blade is partially free to pitch under the action of the aerodynamic and inertia forces so as to reduce the angle of attack and hence the tendency of the blade to stall. Allowed angular swinging of the blade is limited by the presence of two stops. In this way the mathematical model is represented by two systems of equation, each constituted of two equations: momentum balance and hinge moment equilibrium.

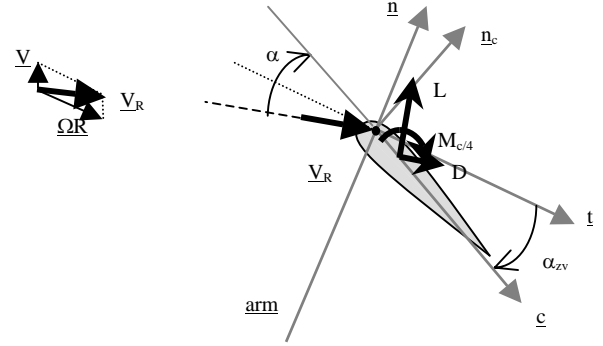


Fig. 6 - Hinge moment equilibrium

For one blade and for the upwind actuator disk

$$\begin{cases} a_u (1 - a_u) = \frac{1}{|\sin \theta_u|} \frac{\sigma}{8\pi} \left(\frac{V_{Ru}}{V_\infty} \right)^2 \{ C_{Lu} (\alpha_{\tan u}, \alpha_{zv}, Re_u) \sin (\theta_u + \alpha_{\tan u}) \\ - C_{Du} (\alpha_{\tan u}, \alpha_{zv}, Re_u) \cos (\theta_u + \alpha_{\tan u}) \} \\ C_{Mc/4} (\alpha_{\tan u}, \alpha_{zv}, Re_u) - C_{Nu} (\alpha_{\tan u}, \alpha_{zv}, Re_u) \cdot (\bar{x}_{c/4} - \bar{x}_{hinge}) \cos \alpha_{zv} \\ - C_{Tu} (\alpha_{\tan u}, \alpha_{zv}, Re_u) \cdot (\bar{x}_{c/4} - \bar{x}_{hinge}) \sin \alpha_{zv} = 0 \end{cases} \quad (5)$$

For the downwind actuator disk

$$\begin{cases} (1 - a_d)(a_d - 2a_u) = \frac{1}{|\sin \theta_d|} \frac{\sigma}{8\pi} \left(\frac{V_{Rd}}{V_\infty} \right)^2 \{ C_{Ld} (\alpha_{\tan d}, \alpha_{zv}, Re_d) \sin (\theta_d + \alpha_{\tan d}) \\ - C_{Dd} (\alpha_{\tan d}, \alpha_{zv}, Re_d) \cos (\theta_d + \alpha_{\tan d}) \} \\ C_{Mc/4} (\alpha_{\tan d}, \alpha_{zv}, Re_d) - C_{Nd} (\alpha_{\tan d}, \alpha_{zv}, Re_d) \cdot (\bar{x}_{c/4} - \bar{x}_{hinge}) \cos \alpha_{zv} \\ - C_{Td} (\alpha_{\tan d}, \alpha_{zv}, Re_d) \cdot (\bar{x}_{c/4} - \bar{x}_{hinge}) \sin \alpha_{zv} = 0 \end{cases} \quad (6)$$

Where α_{zv} is the pitch angle, i.e., the angle between blade chord and the local tangent to the path, Re is the Reynolds number referred to the blade chord, $C_{Mc/4}$ is the airfoil quarter chord pitching moment coefficient, C_N and C_T the blade radial and tangential force coefficient, x_{hinge} and $x_{c/4}$ are, respectively, the floating hinge and blade aerodynamic centre position in percent of the chord. Instantaneous torque, M , and power, P , produced by the blade are given by the moment equilibrium around turbine axis of the radial (N) and tangential (T) forces.

$$M = N(x_{c/4} - x_{hinge}) \cos \alpha_{zv} - T [R - (x_{c/4} - x_{hinge}) \sin \alpha_{zv}] \quad (7)$$

$$P = M \cdot \Omega$$

In the evaluation of the torque produced by a blade (Eq. 7), the aerodynamic forces are applied at the blade aerodynamic centre. It is well known that aerodynamic forces are physically applied in the centre of pressure, whose position along the chord is variable with the incidence angle, but for convenience they are applied in the blade aerodynamic centre considering a transport moment: the airfoil quarter chord pitching moment. In the Eq. 7, such transport moment doesn't appear as it is the case in almost all current literature. It is hypothesized that, because of the flow curvature effects, the pressure distribution upon the airfoil is modified respect to the case of straight flow, determining a shift of the pressure centre towards the aerodynamic centre and so the transport pitching moment is less than that of the straight flow case. Thus, probably, it is correct to neglect its contribution. This aspect is currently being investigated numerically and it will also be experimentally. To obtain the mean torque and mechanical power produced by N_b blades in a revolution it is necessary to average the instantaneous values.

$$M_m = \frac{N_b}{2\pi} \int_0^{2\pi} \left\{ N(x_{c/4} - x_{hinge}) \cos \alpha_{zv} - T \left[R - (x_{c/4} - x_{hinge}) \right] \sin \alpha_{zv} \right\} d\theta$$

$$P_m = \frac{N_b \Omega}{2\pi} \int_0^{2\pi} \left\{ N(x_{c/4} - x_{hinge}) \cos \alpha_{zv} - T \left[R - (x_{c/4} - x_{hinge}) \right] \sin \alpha_{zv} \right\} d\theta \quad (8)$$

To simulate the dynamic performances, we have to resolve only the equation of the moment equilibrium around turbine axis (Eq. 9) for fixed blades or $N_b + 1$ equations for N_b floating blades around their hinge axis (Eqs. 9~10).

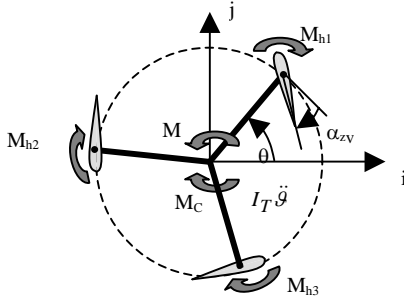


Fig. 7 - Torques on a floating blades turbine

$$I_T \ddot{\theta} = \sum_{i=1}^{N_b} M_i - M_C \quad (9)$$

$$I_p (\ddot{\alpha}_{zv1} - \ddot{\theta}) = M_{h1}$$

$$I_p (\ddot{\alpha}_{zv2} - \ddot{\theta}) = M_{h2} \quad (10)$$

$$I_p (\ddot{\alpha}_{zv3} - \ddot{\theta}) = M_{h3}$$

.....

$$I_p (\ddot{\alpha}_{zvn} - \ddot{\theta}) = M_{hn}$$

Where I_T and I_p are, respectively, the mass moments of inertia of the entire turbine and of the blade; M_i and M_{hi} are the instant torque produced by the single blade about turbine axis and about the blade hinge; M_C is the load torque. Any damping effects are not considered.

COMPARISON BETWEEN DMS NUMERICAL RESULTS AND EXPERIMENTAL DATA

VAWT and VAWT_DYN computer codes, based on the DMS theory, have been developed to predict the steady and dynamic performances

of a cycloturbine with fixed or self-acting variable pitch straight-blades. These codes need the 2D aerodynamic data. Regarding NACA airfoils, data are taken from literature (Paraschivoiu, 2002; Reuss, 1995), while for the HLIFT18 airfoil, TBVOR code (Coiro and de Nicola, 1989; Coiro and Dini, 1997) has been used to generate aerodynamic coefficients values. Airfoil 2D data are corrected, in VAWT and VAWT_dyn codes, to consider three-dimensional effects due to blade finite aspect ratio (Montella and Melone, 2003). To take into account three-dimensional effects, Prandtl's lifting line theory, extended to treat high lift flow, has been used evaluating in this way the 3D lift curve beginning from 2D data. This theory is strictly valid only in the linear zone of the lift curve but with care it is also possible to extend to the non linear conditions. The total blade drag coefficient is the sum of the airfoil drag coefficient, due to skin friction, and the induced drag coefficient. To take into account the interference between the blade and the support arms, a further drag coefficient increment, has been introduced. Moreover a 2D post-stall modelling, based on the Viterna-Corrigan (Eggleston and Stoddard, 1987) correlation method, has been introduced to extend the 2D aerodynamic coefficients to post-stall angle ranges. In Figure 8 the comparison between VAWT code numerical results and experimental data measured on Model A, for different blades number is shown. The power measured is the net rotor power and the tests are carried out with 9 m/s air speed in the DPA wind tunnel for Model A. Comparison of the numerical results with the experimental data shows a good agreement for 3 and 4 blades.

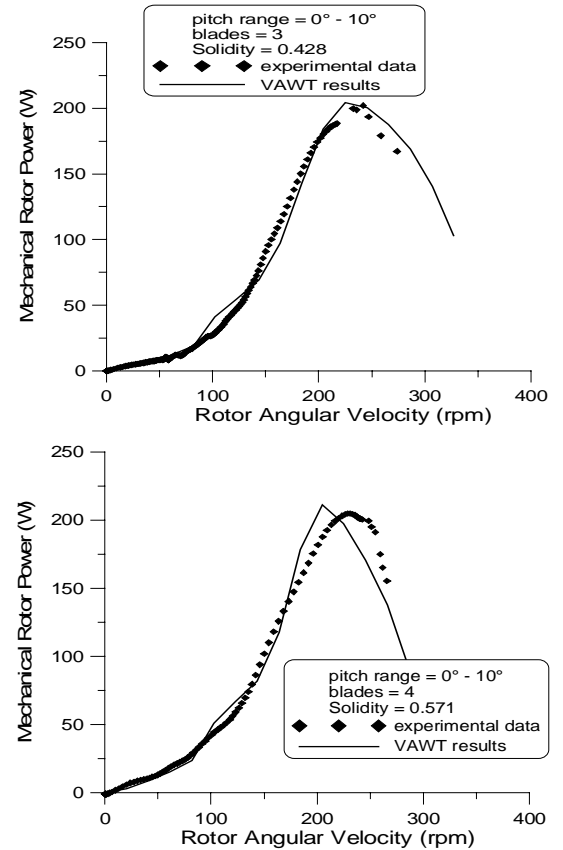


Fig. 8 - Experimental data and VAWT results (Model A)

As it is shown in the figures above, although both turbines have the same maximum power value, the four-blade one is faster to achieve this working condition. This behaviour is expected, because the four-blade turbine has a higher solidity value than the three-blade turbine. Figure 9 shows the comparison between the experimental data measured during

the field tests in water for the *KOBOLD* turbine prototype (Model B) and the VAWT code numerical prediction. The net rotor power coefficient is the ratio between the mechanical shaft power and the theoretical power ($1/2 \rho S V^3$) of the “undisturbed” flow V on the turbine frontal area S ; the tests are carried out with a current speed of 1.5 m/s, but there is an uncertainty around 20% on the real speed value, that is strongly influenced by the location of the current speed meter: this is currently being investigating.

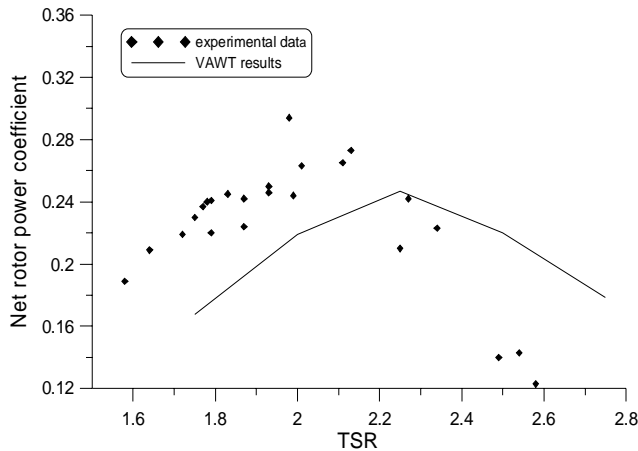


Fig. 9 - Experimental data and VAWT results (*KOBOLD*)

In Figure 10 and Figure 11 are shown experimental data and VAWT_dyn code numerical results referred to the starting condition for the *KOBOLD* turbine prototype.

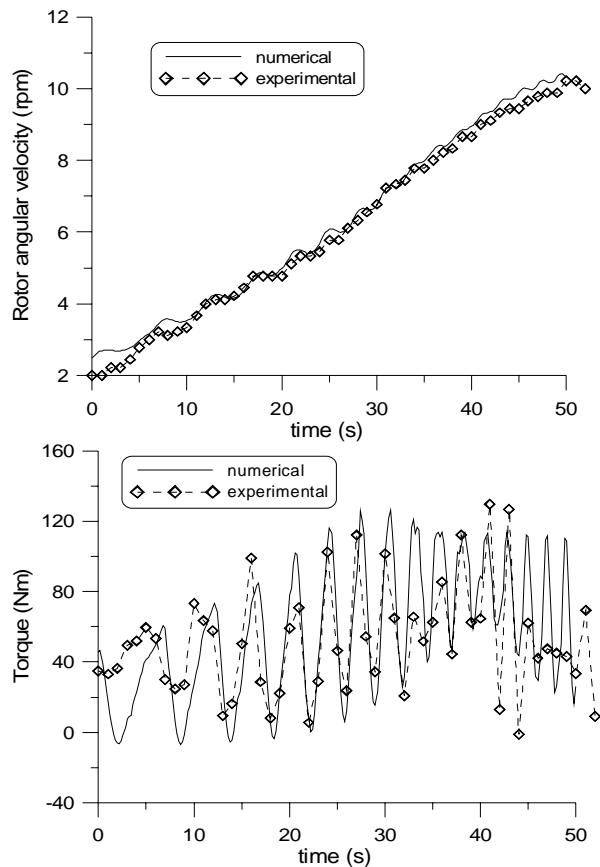


Fig. 10 - Experimental data and VAWT_DYN results (*KOBOLD*)

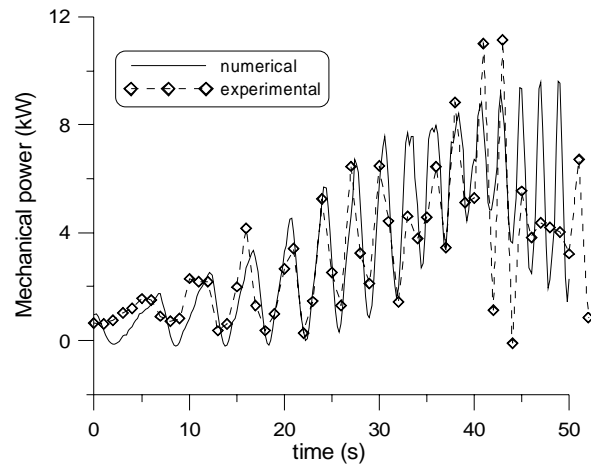


Fig. 11 - Experimental data and VAWT_DYN results (*KOBOLD*)

The time variation of the rotor angular velocity predicted by the code seems to be very accurate, while the rotor torque and power amplitudes are in a good agreement only in the first part of the time range: this is probably due to the uncertain value of the numerical predicted losses. The frequency of the torque and power is instead very well predicted.

VORTEX METHODS: VAT-VOR3D CODE

Streamtube methods are able to correctly predict the turbine performances when rotor blades are not heavily loaded, and for Tip Speed Ratio ($TSR = \Omega R / V_\infty$) not very high. However, for high values of TSR and of solidity such methods do not converge easily and are unreliable and inadequate. Part of these problems may be solved with the use of the so-called “vortex models”, which are based upon the vorticity equations. Such models allow a more realistic modeling of the flow field around and behind the turbine, particularly in those operative conditions characterized by strong blade-wake interference, typical of the high TSR and solidity. The basic concept is to model the blade with a discrete number of lifting surfaces modeled by horseshoe vortex filaments: bound vortex and trailing vortex (Prandtl lifting line theory) (Fig. 12). The production, convection and interaction of these vortex systems springing from the individual blade elements are used to predict the induced velocity at various points in the flow field.

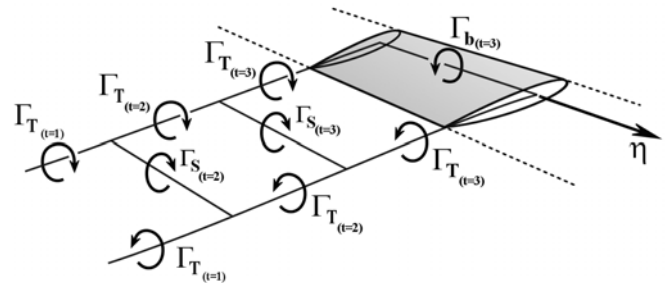


Fig. 12 – Unsteady vortex system of a blade segment

The bound vortex strength (Γ_b) is proportional to the lift acting on the blade segment by the Kutta-Joukowski law.

$$L = \rho V_R \Gamma_b \quad (11)$$

The trailing vortex strength (Γ_T) is related to the change in bound vortex strength along the blade span.

$$\Gamma_T = \frac{d\Gamma_b}{d\eta} \Delta\eta \quad (12)$$

During the blade revolution, the local bound vortex strength changes with time, and, according to the Kelvin's theorem, a spanwise vortex is shed whose strength (Γ_S) is related to the time rate of change of the bound vortex strength.

$$\Gamma_S = \frac{d\Gamma_b}{dt} \Delta t \quad (13)$$

These vortex systems (Bound, Trailing, and Spanwise) induce velocities on different points evaluated by the classic Biot-Savart law, from which the effective angle of attack is obtained and, consequently, the hydrodynamic forces acting on the blades are determined.

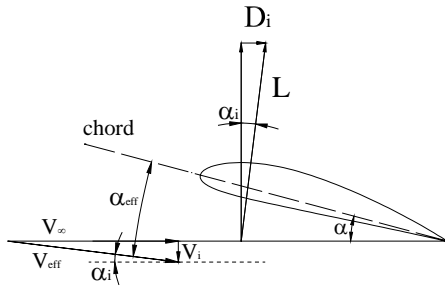


Fig. 13 - Induced velocity by the vortex system and induced drag

The evaluation of the strength of the vortices and the local angle of attack on every blade segment requires an iterative procedure until converged values (of the bound system) are obtained. This model, differently from DMS, automatically takes into account the three-dimensional effects. Strickland first proposed this method. In order to investigate the hydrodynamic behaviour of the vertical axis turbines in many different operating conditions characterized, for example, by high TSR and solidity, it has been developed the code VAT-VOR3D based on the vortex method. This code, derived from VDART code (Strickland) and completely re-written and improved, is able to predict the performances of vertical axis turbines with straight blades (fixed or floating) and curved blades (Darrieus). In the Figure 14 and Figure 15, the numerical prediction by VAT-VOR3D code of the wake of a three blades turbine for different TSR values and a solidity of 0.4 are presented. The continuous line connects the wake points shed by a single blade.

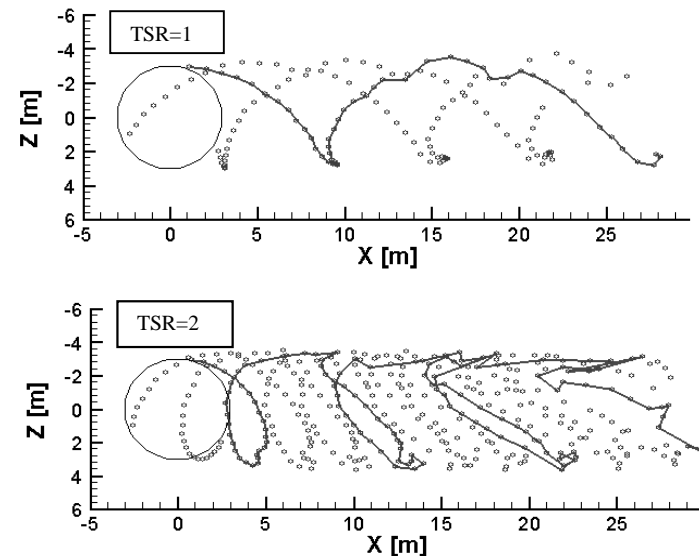


Fig. 14 - Numerical simulation of the wake for different TSR

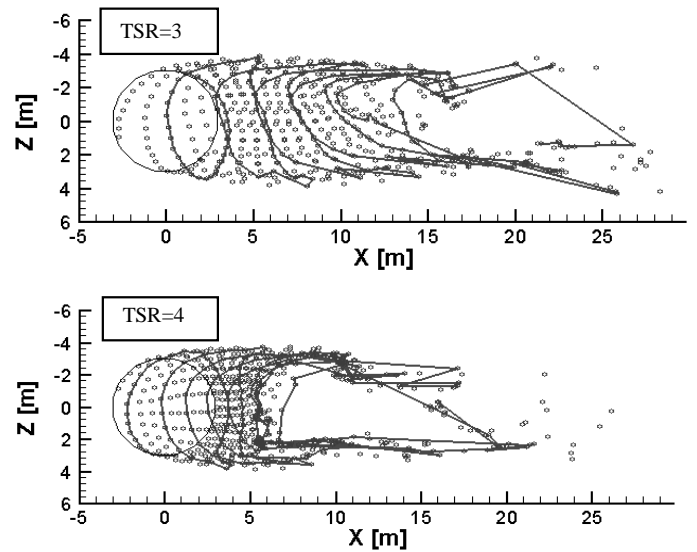


Fig. 15 - Numerical simulation of the wake for different TSR

VAT-VOR3D numerical results have been compared with wake visualizations obtained with water tank tests at Sandia National Laboratories.

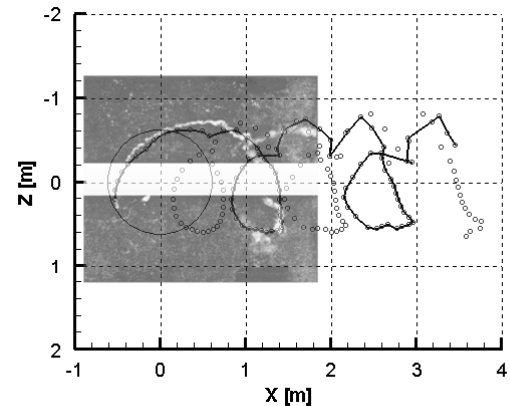


Fig. 16 - Comparison between numerical simulation and experimental results (Strickland, Webster and Nguyen, 1980)

To demonstrate the higher capability of the vortex methods compared to the momentum methods in the operating conditions characterized by high solidity, some comparisons between VAWT code and VAT-VOR3D code results have been made and presented below.

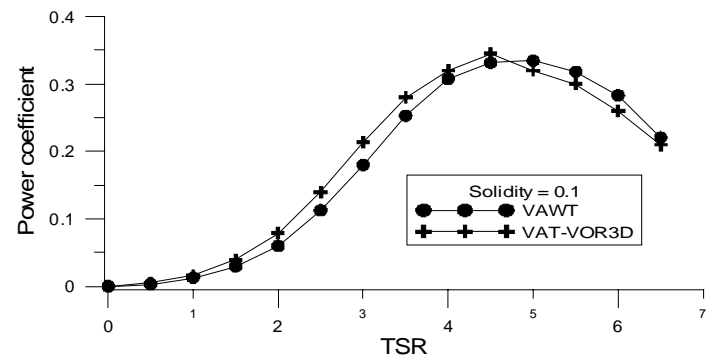


Fig. 17 - Comparison between vortex model and double multiple streamtube model for different solidity values

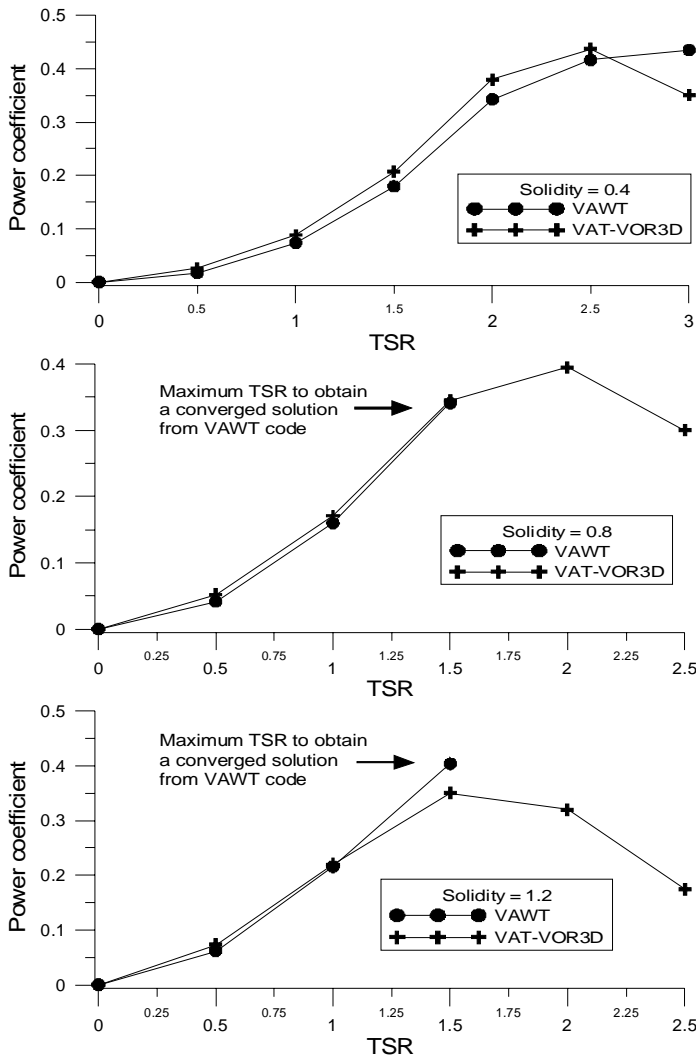


Fig. 18 - Comparison between vortex model and double multiple streamtube model for different solidity values

In graphs of Figure 17 and Figure 18, the limits of the momentum methods models are evident: over a certain TSR and solidity value, the VAWT code is not able to predict turbine performances.

USE OF VAT-VOR3D CODE TO INVESTIGATE THE INTERFERENCE BETWEEN TWO OR MORE TURBINES PLACED SIDE-BY-SIDE

The correct modeling of the interference between two or more turbines placed side-by-side, rotating in the same direction or counter rotating, is very subtle because of the complexity of the physical phenomena involved and, at the same time, it is of the most importance in the optimal design of a plant with a number of turbines placed side-by-side. In particular, it is important to determine the minimal inter-axial distance between the turbines to avoid significant interference effects and performance reduction. The knowledge of the minimal distance is fundamental to place the highest number of turbines in the site without reducing the hydrodynamic performances, or better, to maximize the annual energy that is possible to extract in that site. An extended version of the VAT-VOR3D code has been realized in order to evaluate these effects. In Figure 19 and Figure 20, the preliminary numerical simulations of the wake structure behind two turbines placed side-by-side, rotating in the same direction and counter rotating, are presented.

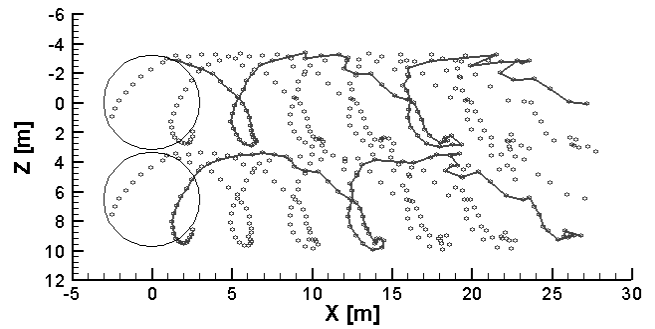


Fig. 19- Numerical simulation of the wake behind turbines rotating in the same direction (solidity=0.4, TSR=1.5)

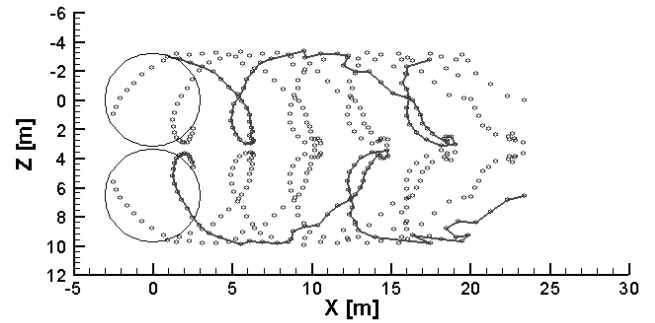


Fig. 20 - Numerical simulation of the wake behind turbines counter rotating (solidity=0.4, TSR=1.5)

It seems that reciprocal influence is not so significant but these aspects are still under evaluation.

FLOW CURVATURE EFFECTS

In the research regarding performances and design of vertical axis turbines, a particularly important aspect is the study of the flow curvature effects. The airfoil mounted on a rotor blade, because of the angular velocity of the rotor, works in a curved flow: each point of the airfoil “sees” a different value of the relative velocity depending on its position along the chord (Hirsch and Mandal, 1984). In almost all numerical methods (both momentum and vortex), it was assumed that the relative flow on a turbine blade is composed of two vectors: the first one is parallel with the free stream flow and the second one is the angular velocity. In every position of the circular path, there is a straight relative velocity \underline{V}_R on the airfoil. This hypothesis is true only for small solidity values for which chord length is much smaller than rotor radius; in this case the airfoil may be considered like a point. A symmetrical airfoil with zero pitch angle, working in curved flow, “works” like a curved airfoil with non zero pitch angle (Migliore, Wolfe and Fanucci, 1980). Flow curvature effects depend on the ratio between the blade chord and rotor radius, i.e. from the solidity. A numerical code, based on a 2D panel method, able to simulate the inviscid hydrodynamics of a generic airfoil in a pure curved flow (only the rotor angular velocity is taken into account) has been developed. In this code special tangential and normal conditions are applied on airfoil surface to take in account the velocities that each airfoil point “sees” during its translation along a curved path. A first result, that confirm the importance of these effects, comes from the analysis of a symmetrical airfoil: the pressure coefficient on the airfoil with zero pitch angle in a curved flow is very different from that on the same airfoil at zero pitch angle in a straight flow with hinge position at 0% chord, as it is shown in Figure 21. It is important to note that the higher negative pressure coefficients (top solid line in the figure) are referred to the lower

surface of the airfoil. So this airfoil, that in a straight flow would show zero lift (C_p curve for the upper and lower surface of the airfoil are identical), in a curved flow shows a negative lift: on the lower surface acts a pressure that is less than the pressure acting on the upper surface, see Figure 22.

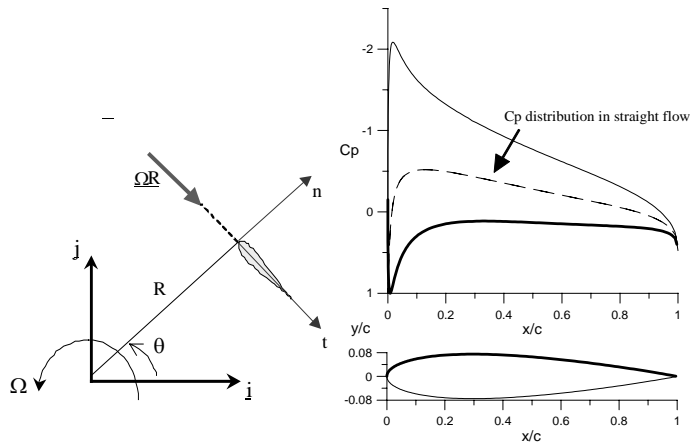


Fig. 21 - Velocity scheme on a blade

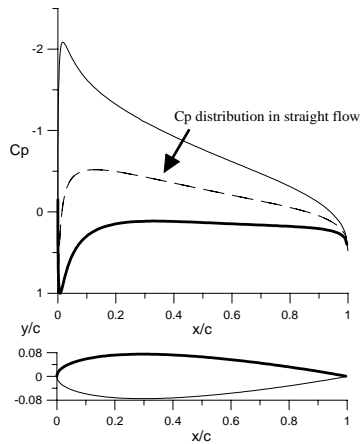


Fig. 22 - Pressure coefficient distribution: 2D panel method results

The effects of the blade hinge position along the chord and of the chord to radius ratio are also under investigation. What appears very clear is that neglecting the curvature effects can lead to erroneous evaluation of the global airfoil's performances. Moreover the airfoil shape should be designed taking in account this important effect and the final shape should somehow nullify the negative torque produced by the curvature effect. This reasoning is particularly valid for high solidity turbines. It is also worth to note that the shape of the pressure coefficient obtained with curved flow is not similar to any C_p 's shape obtained by neither NACA symmetrical airfoil at an angle of attack or by any other NACA non-symmetrical airfoil both set at an angle of attack such to match the maximum negative C_p obtained with curved flow.

CONCLUSIONS

The Double Multiple Streamtube model seems to be accurate enough in predicting performances of the vertical axis turbines especially for solidity values less than 0.5. This model has been implemented in VAWT and VAWT_dyn codes that are then capable of predicting both static and dynamic performances of the turbine with very low computing time. In these codes blade 3D effects have been included as well as arm losses, while it is difficult to predict the losses due to other effects. In the field tests, the accuracy of the tidal speed current measurement could be a problem, because it is difficult to set the current speed-meter in the "real" undisturbed flow, so the measurements have an uncertainty level around the 20%. To overcome typical problems of the DMS model, VAT-VOR3D code, based on a vortex method, has been developed. For low solidity values VAWT and VAT-VOR3D results are very close. For higher solidity values, VAWT code breaks down, because it does not converge, while VAT-VOR3D code is able to evaluate more accurately turbine performances but with a very long computational time. The code, opportunely modified, is also able to simulate the interference of two, or more, turbines placed side-by-side, counter rotating or rotating in the same verse. This aspect, still under investigation, is very important in order to evaluate the correct inter-axial distance between them, avoiding stronger interference effects and performances reduction. Flow curvature effects

on blade's performances have been evaluated by a 2D modified panel method. This preliminary numerical analysis points out that airfoils in curvilinear flow exhibit aerodynamic characteristics very different from what they would in straight flow. Hinge position effects, solidity and curved airfoil effects are currently under investigation and the results of this study will guide the shape of the next airfoils to be employed in vertical axis turbines.

REFERENCES

- Coiro, D.P. and Nicolosi, F. (1998). "Numerical and Experimental Tests for the KOBOLD Turbine," *SINERGY Symposium*, Hangzhou, Republic of China.
- Coiro, D.P. and de Nicola, C. (1989). "Prediction of Aerodynamic Performance of Airfoils in Low Reynolds Number Flows," *Low Reynolds Number Aerodynamics Conference*, Notre Dame, USA
- Coiro, D.P. and Dini, P. (1997). "The Prediction of Aerodynamic Stall Over Wind-Turbine Airfoils," *International Conference on fluid and thermal energy conversion* Yogyakarta, Indonesia.
- Coiro D.P., Nicolosi F., De Marco A., Melone S. and Montella F. (2004) "Dynamic Behavior of a Patented KOBOLD Tidal Current Turbine: Numerical and Experimental Aspects," *4° International Conference on Advanced Engineering Design* Glasgow, UK.
- Eggleston, D.M. and Stoddard, F.S., (1987). "Wind Turbine Engineering Design," Van Nostrand Reinhold Company, New York.
- Hirsch, C. and Mandal, A.C. (1984). "Flow Curvature Effect on Vertical Axis Darrieus Wind Turbine Having High Chord-Radius Ratio," *European Wind Energy Conference*, Hamburg, Germany.
- Kentfield, J.A.C. (1983). "Cycloturbines with freely hinged blades or freely hinged leading edge slats," *Alternative Energy Sources V. Part C: Indirect Solar/Geothermal*, (Editor: T.N. Veziroglu). Amsterdam: Elsevier Science Publishers B.V., p. 71-86.
- Kirke, B.K. and Lazauskas, L. (1993). "Experimental Verification of a Mathematical Model for Predicting the Performance of a Self-Acting Variable Pitch Vertical Axis Wind Turbine," *WIND ENGINEERING*, 17 (2), p. 58-66.
- Lazauskas, L. (1992). "Three Pitch Control Systems for Vertical Axis Wind Turbines Compared," *WIND ENGINEERING*, 16 (5), p. 269-281.
- Migliore, P.G., Wolfe, W.P. and Fanucci, J.B. (1980). "Flow Curvature Effects on Darrieus Turbine Blade Aerodynamics," *Journal of Energy*, 4 (2), p. 49-55.
- Montella, F. and Melone, S. (2003). "Analisi Sperimentale e Numerica del Comportamento Statico e Dinamico di una Cicloturbina ad Asse Verticale," *Aerospace Engineering Graduation Thesis*. Università di Napoli Federico II, Dipartimento di Progettazione Aeronautica, Italy.
- Paraschivou, I. (2002). *Wind Turbine Design with Emphasis on Darrieus Concept*, Ecole Polytechnique de Montreal, Polytechnic International Press.
- Reuss, R.L. et al. (1995). "Effects of Surface Roughness and Vortex Generators on the NACA 4415 Airfoil," *Report: NREL/TP-442-6472*. Golden, Colorado: National Renewable Energy Laboratory.
- Strickland, J.H. (1986). "A review of aerodynamic analysis methods for vertical-axis wind turbine," *Fifth ASME Wind Energy Symposium*, SED-Vol.2 edited by A.H.P. Swift.
- Strickland, J.H., Webster, B.T. and Nguyen T. (1980). "A vortex Model of the Darrieus Turbine: an Analytical and Experimental Study," *SAND79-7058 Contractor Report*.
- Templin, R.J. (1974). "Aerodynamic Performance Theory for the NCR Vertical Axis Wind Turbine," *Report: LTR-LA-160*. National Research Council of Canada.